JOURNAL OF GEOPHYSICAL RESEARCH, VOL. 114, B06407, doi:10.1029/2008JB006239, 2009

GRACE-derived ice-mass variations over Greenland by accounting for leakage effects

O. Baur,[1] M. Kuhn,[2] and W. E. Featherstone[2]

Received 5 December 2008; revised 25 March 2009; accepted 4 May 2009; published 23 June 2009.

[1] After more than 6 years in full operational mode, the Gravity Recovery and Climate Experiment (GRACE) satellite mission provides the opportunity to derive global secular mass changes from space-geodetic observations. Crucial for a reliable estimate of secular mass changes is the ability to correct for spectral and spatial leakage effects. In order to account for any leakage signal, we present and apply a four-step procedure, including a validation step based on forward gravity modeling. Most notably, our method is characterized by the separation and quantification of individual leakage sources. We test and apply our procedure to the Greenland area, which exhibits the strongest secular trend signal. On the basis of simulation studies, we demonstrate that leakage-out effects are dominant for the Greenland area, and if not accounted for, mass-change rates will be underestimated. Analyzing time-variable GRACE gravity fields covering 6 whole years (August 2002 to July 2008, inclusive), we estimate the ice-volume loss over Greenland to be -177 ± 12 km^3 a^{-1}. This value is the average derived from monthly gravity field models provided by CSR, GFZ and JPL, with individual contributions of -242 ± 14 km^3 a^{-1}, -194 ± 24 km^3 a^{-1} and -96 ± 23 km^3 a^{-1}, respectively. We highlight that without taking leakage effects into account, mass-change amplitudes over Greenland are reduced by a factor of 2. Despite the rather large spread of the results among GRACE processing centers, our results are in better agreement with the findings from alternative GRACE analysis methods and InSAR observations.

Citation: Baur, O., M. Kuhn, and W. E. Featherstone (2009), GRACE-derived ice-mass variations over Greenland by accounting for leakage effects, *J. Geophys. Res.*, *114*, B06407, doi:10.1029/2008JB006239.

1. Introduction

[2] Since 2002, the GRACE (Gravity Recovery And Climate Experiment) twin-satellite mission has been providing time-variable gravity field information from space [e.g., *Tapley et al.*, 2004a, 2004b]. The data enable spatio-temporal mass changes to be monitored, providing important input to various (geo)sciences, most notably in the context of global climate and sea level change. The anticipated mission lifetime of 5 years has in the meantime been extended until late 2010 [*Chen et al.*, 2006c]. This will allow for the derivation of more stable estimates of seasonal, interannual and secular (surface) mass variations by analyzing residual gravity field solutions taken with respect to longer-term averages.

[3] When the temporal resolution of GRACE was restricted to only a couple of years, the mission mainly mapped annual and interannual hydrological variations such as surface water and groundwater changes in the major river basins [e.g., *Tapley et al.*, 2004b] or significant ice-mass changes in polar areas [e.g., *Velicogna et al.*, 2005]. In this framework, most studies focused on the Amazon-Orinoco watershed, as it is the largest drainage basin and also exhibits the largest annual signal observed by GRACE [e.g., *Tapley et al.*, 2004b; *Ramillien et al.*, 2005; *Han et al.*, 2005a]. An increasing number of other investigations have applied GRACE data to derive ocean mass-change patterns [e.g., *Chambers*, 2006b] or to map ocean currents [e.g., *Dobslaw and Thomas*, 2007]. Moreover, by combining GRACE with satellite altimetry, it is possible to compute steric sea level change effects over the world's oceans [e.g., *Chambers*, 2006a; *Lombard et al.*, 2007].

[4] With the GRACE mission now operating for over 6 years, more studies are being directed toward secular changes over currently ice-covered areas, most notably the polar ice sheets. Changes of mass balance over the Antarctic ice sheets have been reported by *Chen et al.* [2006c], *Velicogna and Wahr* [2006a] and *Ramillien et al.* [2006]. Also, on the basis of GRACE data, significant ice melting of the Alaskan glaciers has been shown by, e.g., *Chen et al.* [2006a] and *Tamisiea et al.* [2005]. Considerable recent deglaciation of the Greenland ice sheets has been confirmed by *Velicogna and Wahr* [2005], *Chen et al.* [2006b], *Luthcke et al.* [2006], *Ramillien et al.* [2006] and *Velicogna and Wahr* [2006b], with possible accelerated melting in the recent past [*Chen et al.*, 2006b; *Luthcke et al.*, 2006]. Scrutinizing the estimates of these studies for the total ice-volume loss over Greenland reveals a rather large spread

[1] Institute of Geodesy, Universität Stuttgart, Stuttgart, Germany.
[2] Western Australian Centre for Geodesy and Institute for Geoscience Research, Curtin University of Technology, Perth, WA, Australia.

0148-0227/09/2008JB006239$09.00

Table 1. Available Monthly GRACE Gravity Field Solutions in the Time Span August 2002 to July 2008 (Inclusive)

Processing Center	Spectral Resolution	No. of Solutions	Data Gaps
CSR	60	71	6/03
GFZ	120	67	9/02, 12/02, 1/03, 6/03, 1/04
JPL	120	70	8/02, 6/03

among the different studies, ranging from -82 ± 28 km^3 a^{-1} to -248 ± 36 km^3 a^{-1}, well exceeding the formal errors given. This has prompted this study in an attempt to explain the discrepancies among the procedures and data used.

[5] A major obstacle to deriving reliable mass-change rates from GRACE is the correction for leakage effects. In terms of GRACE-derived (surface) mass changes, leakage occurs because of both the restricted spectral resolution of gravitational field estimates and spatial averaging [e.g., *Chen et al.*, 2006c]. Basically, spectral leakage emerges when high-frequency signals or errors are mapped into lower frequencies, thus introducing artificial low-frequency signals that are not present in reality. In the spatial domain, leakage manifests as signals spreading spatially, thus not being concentrated directly over the area of mass variation, but also leaking to the surrounding region [e.g., *Chen et al.*, 2006b], theoretically over the whole globe. The reliability of mass-change estimates depends mainly on the ability to identify, quantify and remove these leakage effects. The possibility of improper correction for leakage effects may explain the bulk of the large discrepancies among GRACE-derived ice-mass balance results.

[6] Our primary objective in this study is the systematic isolation and correction for any leakage effects that have a significant impact on GRACE-derived mass-change results. We develop and apply a four-step computation procedure that accounts for leakage effects and show that neglecting spectral leakage can introduce substantial biases. In particular, the procedure is characterized by the separation and quantification of both signal leaking out of the region of interest and signal leaking into the region of interest. In order to distinguish these two effects, we refer to the former as leakage-out signal and the latter as leakage-in signal. Most notably, we attend to the systematic classification of the complex behavior of leakage effects, which has never been addressed in detail before.

[7] The greatest secular trend observed by GRACE is located over Greenland, showing this area to be one of the most affected, hence our choice to use it as a case study. On the basis of our computation procedure, we provide a detailed study on the leakage-out signal for ice-mass changes over the Greenland ice sheet and leakage-in signals from all major mass changes in the Arctic region (including GIA signals over the Canadian Shield and Fennoscandia and glacier melt over Alaska). We recalculate the magnitude of the total ice-mass change using 6 whole years of GRACE data (August 2002 to July 2008, inclusive). We also investigate three independently estimated series of monthly GRACE solutions provided by (1) the Center for Space Research (CSR), University of Texas at Austin (2) the GeoForschungsZentrum (GFZ) Potsdam, and (3) the Jet Propulsion Laboratory (JPL).

2. Data and Methodology

2.1. GRACE Monthly Solutions

[8] Typically, static 30-day GRACE gravity field estimates ("monthly solutions") are released to the public in terms of fully normalized spherical harmonic coefficients $\bar{c}_{lm}$ and $\bar{s}_{lm}$ [e.g., *Heiskanen and Moritz*, 1967] of the Earth's external gravitational potential. Moreover, monthly residual gravity field solutions are expressed by the residual spherical harmonic coefficients

$$\Delta\bar{c}_{lm} = \bar{c}_{lm} - \bar{c}_{lm}^{\text{mean}} \quad \text{and} \quad \Delta\bar{s}_{lm} = \bar{s}_{lm} - \bar{s}_{lm}^{\text{mean}}, \tag{1}$$

where $\bar{c}_{lm}^{\text{mean}}$ and $\bar{s}_{lm}^{\text{mean}}$ represent static mean parameters such as long-term averages.

[9] We use release four (RL04) GRACE-only gravity field estimates provided by CSR, GFZ and JPL. Each monthly solution consists of a set of coefficients complete up to degree and order 60 (CSR) and 120 (GFZ, JPL). In order to avoid aliasing effects of strong seasonal signals falsifying our secular-change estimates, we choose the total timespan of the gravity field series to cover 6 whole years, ranging from August 2002 to July 2008 (inclusive). Table 1 outlines the sequences used. Data gaps occurred for a few months, when the GRACE satellites passed through orbital resonances so could not fully resolve the gravity field [see *Wagner et al.*, 2006]. In order to remove correlated errors, we apply spectral-domain filtering of GRACE (residual) spherical harmonic coefficients according to *Swenson and Wahr* [2006].

2.2. Mass Change in Terms of Equivalent Water Thickness

[10] Vertically integrated mass changes are typically approximated by surface mass-densities [*Wahr et al.*, 1998]. As a function of the residual coefficients in equation (1) they become

$$\Delta\bar{\sigma}(\lambda,\varphi) = \frac{2\pi a\rho_{\text{ave}}}{3}\sum_{l=0}^{L}\frac{2l+1}{1+k_l}W_l\sum_{m=0}^{l}\bar{P}_{lm}(\sin\varphi) \cdot (\Delta\bar{c}_{lm}\cos m\lambda + \Delta\bar{s}_{lm}\sin m\lambda). \tag{2}$$

Furthermore, the simple relation

$$\Delta\bar{\nu}(\lambda,\varphi) = \frac{\Delta\bar{\sigma}(\lambda,\varphi)}{\rho_{\text{w}}} \tag{3}$$

transforms surface mass-densities to equivalent water thickness (EWT) values.

[11] In equations (2) and (3), (λ, φ) denote spherical polar coordinates with λ East longitude and φ latitude. GM is the geocentric constant, a is the major semiaxis of a reference ellipsoid and $L = l_{\max}$ is the maximum spherical harmonic degree (spectral resolution). ρ_{ave} denotes the average mass-density of the solid Earth and ρ_{w} the mass-density of freshwater. The numerical values used in this study are $\rho_{\text{ave}} = 5517$ kg m^{-3}, $\rho_{\text{w}} = 1000$ kg m^{-3} respectively. The degree-dependent load Love numbers k_l are taken from *Farrell*

[1972] for the Gutenberg-Bullen model. The latitude-dependent functions $\bar{P}_{lm}(\sin\varphi)$ represent the 4π-normalized associated Legendre functions of the first kind [e.g., *Heiskanen and Moritz*, 1967].

[12] Moreover, equation (2) accounts for spatial averaging in terms of Gaussian smoothing [*Wahr et al.*, 1998], damping errors of high-degree GRACE-derived coefficients using a Gaussian isotropic filter. The filter itself is characterized by the smoothing radius R. As the high-degree terms are amplified by the factor $2l + 1$, high-frequency errors significantly affect the accuracy of surface mass-density estimates. Hence the smoothing coefficients W_l in equation (2) down-weight the short wavelength parts. For the computation of the weighting coefficients, we use the recursion relations given by *Jekeli* [1981].

[13] The choice of the smoothing radius R depends on the balance between the attenuation of high-frequency GRACE measurement errors and the intensification of spectral leakage errors. The former increase with decreasing smoothing radius, whereas the latter augments with increasing R. As shown in the study by *Swenson et al.* [2003], the minimum of the sum of both errors typically occurs in the range R = 200 km–600 km. As such, we apply Gaussian smoothing ranging from R = 200 km to R = 600 km.

[14] Besides the Gaussian isotropic filter, a variety of alternative smoothing kernels have been proposed [e.g., *Swenson and Wahr*, 2002; *Swenson et al.*, 2003; *Han et al.*, 2005b]. Although the arguably more sophisticated filters are designed to simultaneously minimize GRACE measurement and spectral leakage errors, we adopt Gaussian smoothing for our investigations because it provides nearly identical results to alternative, albeit seemingly more sophisticated, techniques [*Chambers et al.*, 2007]. Moreover, the choice of filter does not impact on the philosophy of our approach, and others may wish to choose to experiment with alternative filters in conjunction with our proposed method.

2.3. Glacial Isostatic Adjustment Effects

[15] Secular trends in ice-mass changes are superposed by the continuing viscoelastic response of the Earth's crust and upper mantle due to past glacial loads, referred to as glacial isostatic adjustment (GIA) [e.g., *Peltier and Andrew*, 1976]. For the comparatively short GRACE lifetime (6 years versus ~12,000 years since the last glacial maximum), the GIA signal can be assumed to be linear in time [*Swenson et al.*, 2003]. It is mainly concentrated over the Canadian Shield, Fennoscandia, Greenland and Antarctica, i.e., regions with strong glaciation at the end of the last glacial maximum.

[16] Since GRACE measurements are insensitive to the vertical distribution of mass, it is impossible to separate/discriminate between gravity signals caused by ice-mass changes and signals caused by GIA-induced mass redistribution, or other causes. Therefore, if not corrected, GIA signals will manifest as an apparent ice-mass change.

[17] Unfortunately, there are still some open issues in the context of GIA modeling. Basically, the models depend on assumptions of the ice-load history and mantle viscosity, leading to considerably large error bounds [*Chen et al.*, 2006c; *Velicogna and Wahr*, 2006a]. Therefore, because of the "controversy" in GIA modeling, the mass-change rates given in this paper are not corrected for GIA effects. It is not our intention to investigate the impact of different GIA models. Instead, like the case of the filter options, we leave it to others to choose their preferred model. Nevertheless, here we give the order of magnitude of the GIA effect for the whole of the Greenland area. According to *Velicogna and Wahr* [2006b], the correction is about -8 ± 21 km^3 a^{-1}, which is almost negligible when compared to secular mass-change estimates that are more than one order of magnitude larger.

3. Removing Leakage

3.1. Global Secular Mass Changes

[18] On the basis of monthly residual gravity field solutions, we derived global GRACE-observed secular mass changes in terms of EWT over the exact 6-year period following the procedure as outlined in section 2.2. Figure 1 shows our estimates for the globally distributed variations expressed in terms of EWT (see equation (3)), evaluated on a spherical $1^\circ \times 1^\circ$ grid.

[19] While showing very similar spatial patterns, the solutions from the different GRACE processing centers (CSR, GFZ and JPL) vary considerably in the magnitude of the derived secular mass changes. The most prominent positive features in Figure 1 are located over the Canadian Shield and around the Amazon-Orinoco watershed in South America. As outlined in section 2.3, the former have to be attributed to GIA-induced land uplift. The latter suggest secular surface water and groundwater gain in the Amazon-Orinoco river basin. Prominent negative signals occur over Greenland, Alaska and Antarctica. Compared to all other regions around the globe, the signal over Greenland is by far the strongest in magnitude.

[20] For the interpretation of Figure 1, it has to be kept in mind that because of the limited spectral resolution of GRACE, reliable results of mass changes can only be derived in regions with dimensions of more than several hundred kilometers [*Tapley et al.*, 2004a].

[21] In this study we will focus on mass changes over Greenland, which we trace back to secular ice-mass decline of the Greenland ice sheet. However, our mass estimation procedure can also be applied to other regions, both in the cryosphere and elsewhere.

3.2. Leakage Problem and Its Proposed Solution

[22] The major problem for the computation of mass variations from the GRACE patterns in Figure 1 arises because of leakage effects. As highlighted in Figure 2, leakage affects the determination of mass-change rates over Greenland in two different ways. On the one hand, mass change over Greenland manifests as a signal spreading out over the landmass area (practically, the signal spreads over the whole globe, indicated by the dashed red lines). From the Greenland point of view (e.g., the area over which mass changes are occurring), the signal leaks out, hence we refer to it as leakage-out signal. It has to be restored back into the region of interest.

[23] On the other hand, mass change at a location outside Greenland, e.g., over the Canadian Shield, also propagates into a signal spreading over the whole globe (indicated by

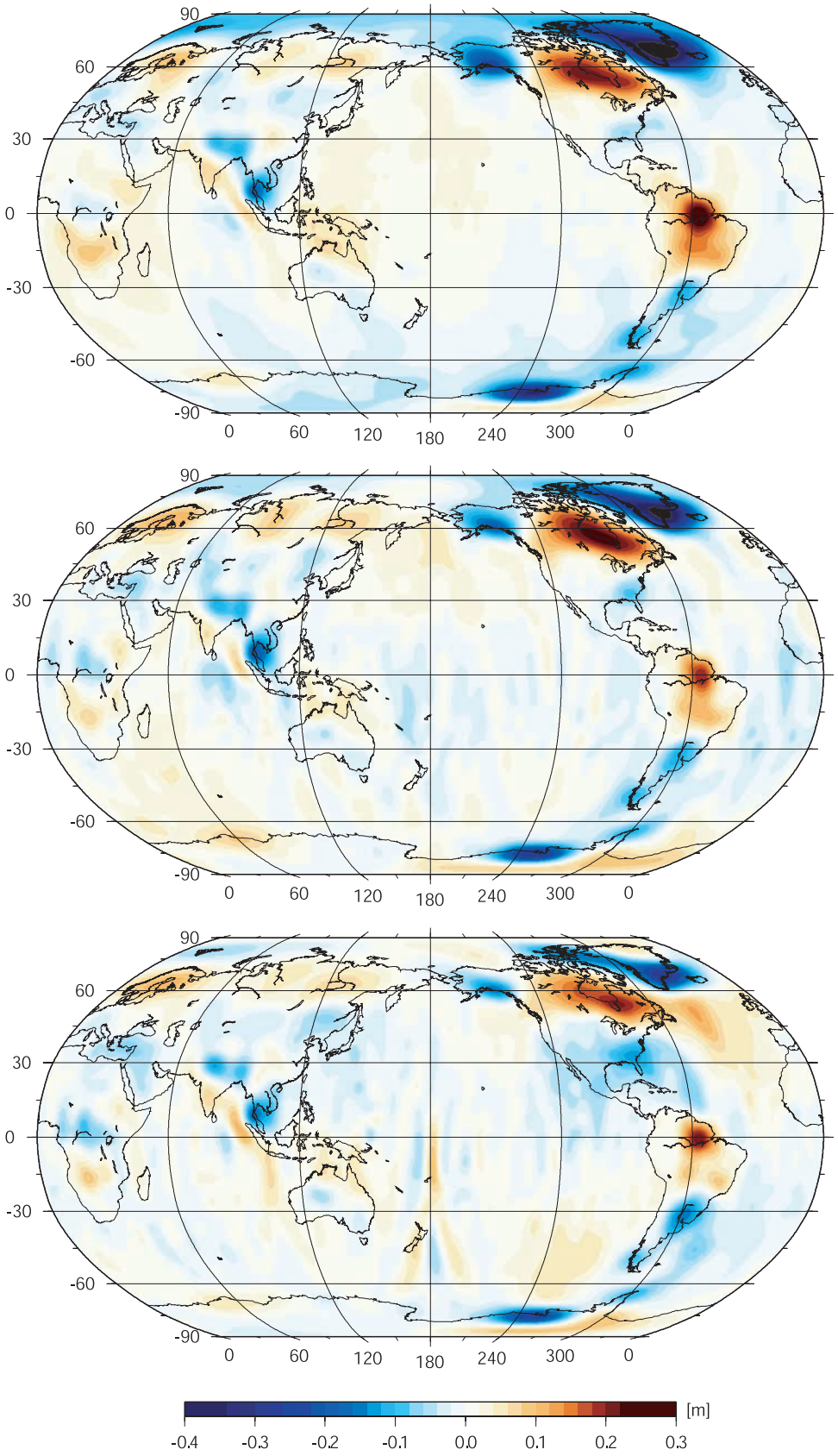

Figure 1. Global maps of GRACE-derived secular equivalent water thickness variations from August 2002 to July 2008 (inclusive). (top) CSR, (middle) GFZ, and (bottom) JPL. Gaussian smoothing applied with a R = 500 km radius [Robinson projection].

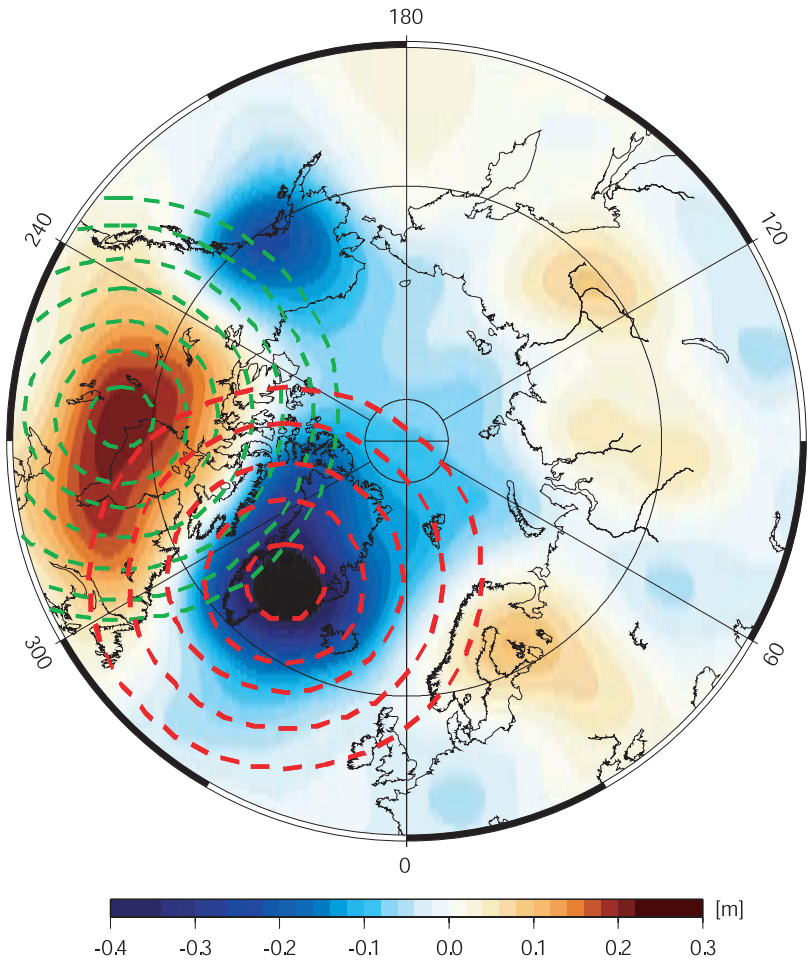

Figure 2. Nature of leakage-out (dashed red lines) and leakage-in (dashed green lines) signals from the Greenland point of view [Azimuthal projection].

the dashed green lines in Figure 2), and hence has an impact on the mass-change estimation process over Greenland. From the Greenland point of view, the signal leaks in, thus we refer to it as leakage-in signal. It has to be reduced from the region of interest. We denote the sources generating leakage-in signals as "disturbing sources".

[24] Basically, any disturbing source contributes to the overall signal over Greenland. However, the impact strongly reduces with increasing distance, according to Newton's law of gravitation. In Figures 1 and 2, the strongest signals close to Greenland are located over Alaska, the Canadian Shield and Fennoscandia. Hence these signals mainly influence the mass-change estimation process over Greenland in terms of leakage-in effects.

[25] Our ice-mass change estimates (applied to Greenland) are based on a four-step procedure (Figure 3), which accounts for spectral leakage effects by the combination of extended spatial filters, followed by "calibration" in terms of comparison with forward gravitational modeling results. The procedure provides magnitudes of ice-mass variations with their corresponding error bounds. While similar to the approach in the study by *Chen et al.* [2006b], the major difference is that we use solely GRACE results to delineate the broad areas of ice-mass change rather than additional information from remote sensing.

[26] First, we describe our four-step procedure in order to restore leakage-out signals. Later, we explain how to quantify leakage-in contributions of individual disturbing sources using the same four-step procedure.

3.2.1. Step 1

[27] The spatial mass distribution and the total mass change M_1 are extracted from Figure 1, only considering land areas (i.e., Greenland in Figure 3, or more generally the area of interest). Neglecting any leakage effects will usually lead to an underestimation or overestimation of the total mass change (underestimation in the case of Greenland), therefore only providing approximate information.

3.2.2. Step 2

[28] This step takes an extended area into account in order to derive a more realistic estimate, M_2, for the total mass change, but keeping the spatial distribution as obtained in step 1. As indicated in Figure 4, we use selected (signal strength) isolines as delineation, but the procedure can be applied to any arbitrary extended area. As will be shown later, our procedure is largely insensitive to the selection of the isoline. However, we recommend a selection in the way

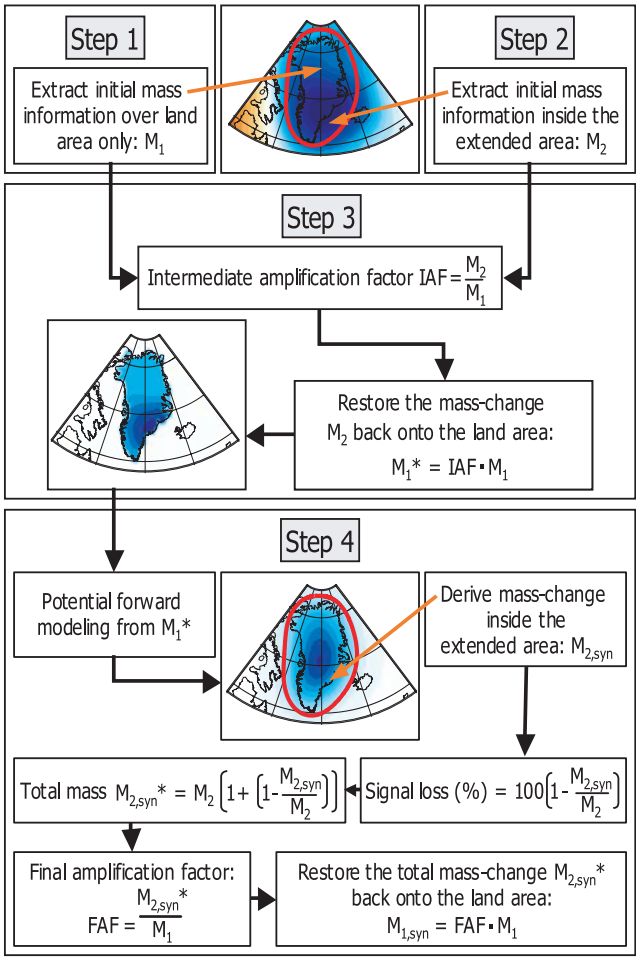

Figure 3. Four-step procedure for estimating ice-mass change magnitudes and geometries, with examples for Greenland.

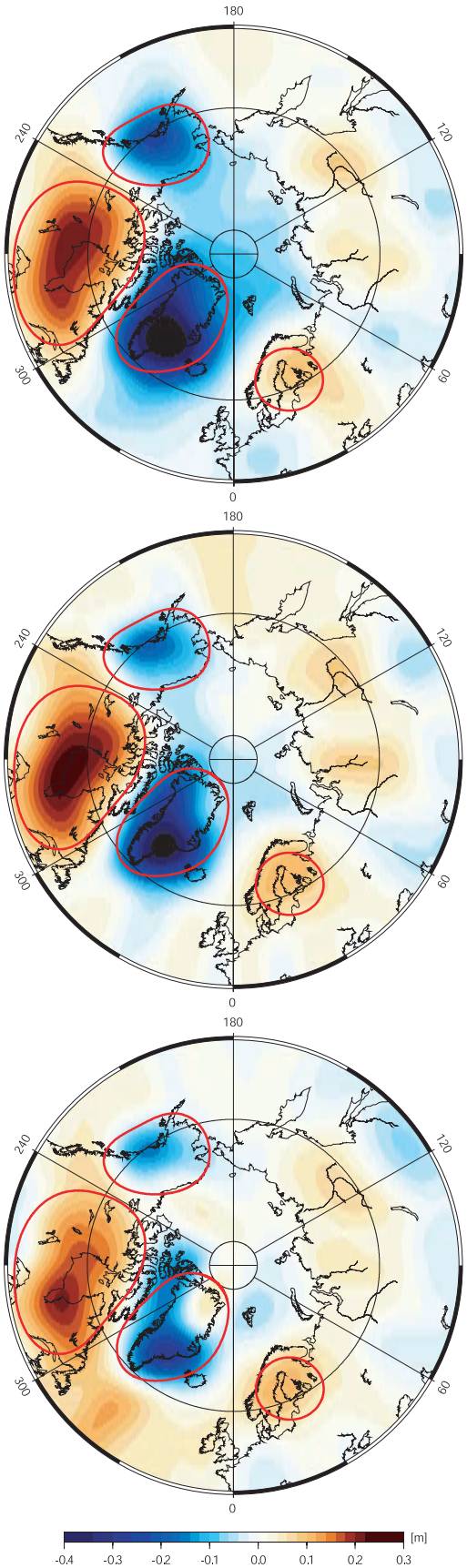

Figure 4. GRACE-derived equivalent water thickness variations from August 2002 to July 2008 (inclusive) over the Arctic region. (top) CSR pattern, (middle) GFZ pattern, and (bottom) JPL pattern. Gaussian smoothing applied with a R = 500 km radius. Red isolines enclose the areas of main mass variation [Azimuthal projection].

that other major mass sources are excluded from the extended area (e.g., the Canadian Shield when focusing on Greenland) so that the estimate M_2 is indeed more realistic then M_1.

3.2.3. Step 3

[29] The results of steps 1 and 2 are combined by defining a mass distribution over the area of interest that follows the spatial distribution obtained in step 1 but satisfies the mass change M_2. The combination is performed by applying an *intermediate amplification factor* (IAF), the relation between M_1 and M_2, to the mass distribution extracted in step 1 (see Figure 3). Depending on the selection of the extended area, the rescaling provides an improved mass distribution, as part of the leakage-out signal has been restored back into the region of interest. The improved pattern is the input for

Table 2. Volume-Change Input Values for the Closed-Loop Simulation Studies

Region	Origin	Volume-Change (km^3)
Greenland	deglaciation	−500
Alaska	deglaciation	−300
Canadian Shield	glacial isostatic adjustment	+850
Fennoscandia	glacial isostatic adjustment	+100
Sum	–	+150

the forward gravity modeling technique applied in the final step.

3.2.4. Step 4

[30] The aim here is to validate and essentially "calibrate" the result of step 3 using a closed-loop forward gravity modeling technique, finally providing the "exact" leakage-out effect. This is done by analyzing the gravitational potential signal obtained by gravity forward modeling of the mass-change distribution from step 3. The forward-modeled potential signal is used to retrieve the total mass-change $M_{2,\mathrm{syn}}$, using the same extended area as chosen in step 2.

[31] The ratio between the forward-modeled total mass-change estimate $M_{2,\mathrm{syn}}$ and the estimate M_2 from step 2, expressed here as $(1 - M_{2,\mathrm{syn}}/M_2)$, reveals the amount of signal loss inherent in the computation procedure for the extended area. Furthermore, it validates the procedure itself. We combine the amount of signal loss and the IAF from step 2 in the *final amplification factor* (FAF) (see Figure 3), which has to be applied to the mass distribution extracted in step 1 to fully restore the leakage-out effect onto the area of interest.

[32] We acknowledge, that steps 2 and 3 can be considered as intermediate steps. In principle, step 4 can directly be applied to the results of step 1. However, we chose to include steps 2 and 3, so as to incorporate more realistic mass-change estimates as the input for the forward modeling procedure in step 4.

3.2.5. Leakage-in

[33] The computation of leakage-in effects follows the same procedure. There is only one difference: After having isolated the individual disturbing source (by applying steps 1 to 4 to that particular source), its impact on the region of interest has to be determined. For each disturbing source separately, this is done by evaluating the magnitude of the restored mass-change signal in the region of interest. In other words: Leakage-out from, say, region A into region B is nothing else but leakage-in into region B from region A.

4. Simulation Studies

[34] In order to test the feasibility and prove the correctness of our procedure in section 3.2, we perform two closed-loop simulation studies. Both studies are based on a priori known mass variations and volume changes near the Arctic. In particular, we consider the major mass changes as seen by GRACE. According to Figure 4, they are located over Greenland, Alaska, the Canadian Shield and Fennoscandia. Table 2 presents the numerical volume-change input values. Although somewhat arbitrarily fixed, we have chosen them to be close to the total changes as obtained by GRACE.

[35] The variations in Table 2 are forward modeled (by Newton integration) in order to obtain the corresponding change in gravitational potential. The forward modeled potential is first evaluated on a global 15-arc-min by 15-arc-min grid and subsequently converted by spherical harmonic analysis to a set of fully normalized spherical harmonic coefficients up to degree and order 120. From the gravitational potential values (given in terms of an harmonic series expansion), the computation of EWT values follows the same procedure as outlined in section 2.2. In terms of spatial averaging, we apply Gaussian smoothing with smoothing radius R = 500 km. We apply our procedure to the simulated EWT patterns. Finally, we compare the resulting volume-change magnitudes with the initial input values in Table 2.

4.1. A Simple Simulation (Greenland Ice Shield Only)

[36] The first study considers only one mass-change signal located over Greenland. The spatial distribution of the initial variations is chosen such that the strongest signal in magnitude is at the southeast coast of Greenland. Thus, in this simple example, we totally neglect disturbing influences. As a consequence, no leakage-in effects occur at all. This configuration is far from reality, but it gives an important insight in the procedure's performance regarding its ability to restore leakage-out effects. The gravitational potential forward modeling result, and hence, the input for the procedure, is given in Figure 5. The initial total volume-change magnitude is -500 km^3. Note that this value can be chosen arbitrarily within the closed-loop investigation.

4.1.1. Steps 1–3

[37] Applying the first step of the procedure in section 3.2 to the pattern in Figure 5 leads the volume-change over Greenland to become -305.2 km^3. This value is much lower than the input value (-500 km^3) due to leakage-out.

[38] The second step evaluates the volume-change magnitude within an extended area, enclosing both the landmass area and regions affected by leakage-out signals. As we introduced no disturbing masses for this first simulation, the definition of the extended area is arbitrary. With regard to the more advanced study in section 4.2 and GRACE analysis in section 5, however, we choose the delineation so as to keep disturbing influences small. Hence, aside from the landmass itself, the extended area contains coastal areas only.

[39] Figure 6 displays four selected extended areas. They represent the mass-change contour lines according to the -0.04 m, -0.05 m, -0.06 m and -0.07 m isolines, expressed in terms of EWT. Although the delineations do not differ a lot geometrically, according to Table 3 (second column), the resulting volume-change magnitudes increase considerably with an enlarged extended area. The third column in Table 3 presents the IAF as the ratio between the estimate within the extended area and the value obtained over the Greenland landmass. Naturally, the larger the extended area, the larger the IAF. As a check, we also derived the mass change for the signal spreading over the whole globe and could completely restore the input

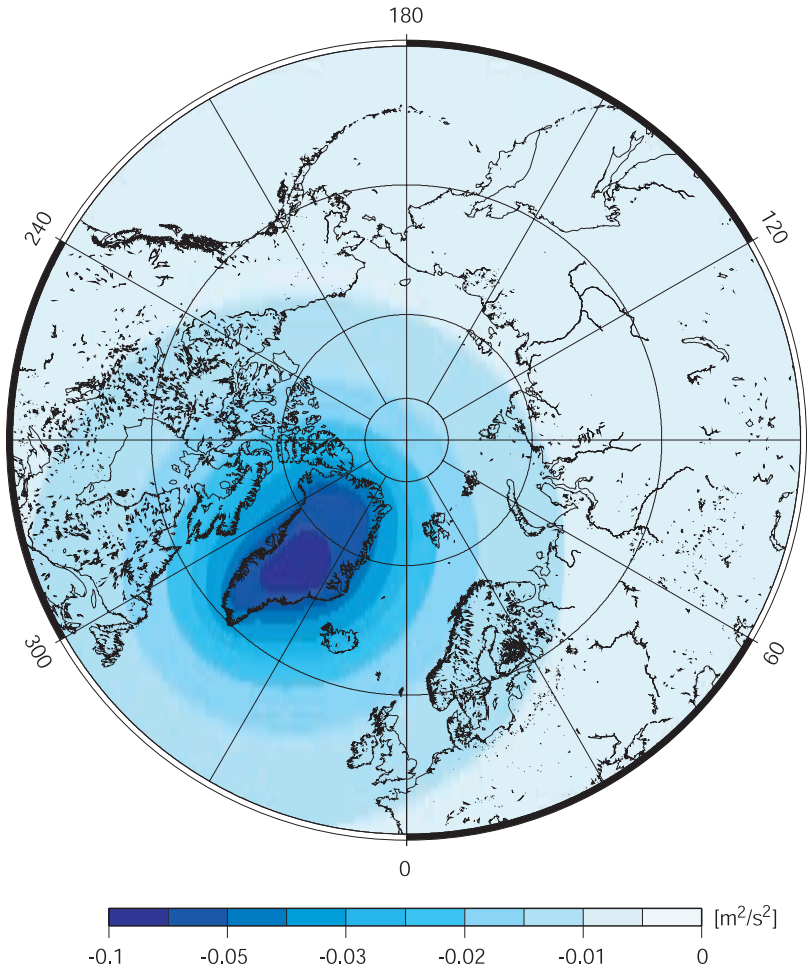

Figure 5. Input for the first simulation study: forward modeled potential signal [Azimuthal projection].

mass, which is possible here as no disturbing masses are considered.

4.1.2. Step 4

[40] The IAF allows restoration of the leakage-out signal inside the extended area back onto the land area, see section 3.2. The resulting pattern is used in the last step of the procedure to quantify the amount of signal leaking beyond the limited delineation of the extended area. The signal loss, hence the additional leakage-out signal that has not been considered so far, turns out to be in the range of 4% to 23% (fourth column in Table 3). Adding the signal loss to the volume-change estimate inside the extended area results in the total volume-change $M_{1,\mathrm{syn}}$. From these values, the computation of the FAF is straightforward. Most notably, the FAF does not depend on the choice of the extended area. This important fact makes the routine robust toward arbitrary definitions of the extend area.

[41] This closed-loop simulation allows us to quantify the model errors by comparison of the final results with the initial input value (-500 km^3). The model errors vary between 0.9% and 1.6%. Hence leakage-out signals can (almost) be fully restored. The total estimated leakage-out effect is given by the difference between the mass change within the extended area and the result over landmass, added to the signal loss. On the other hand, the true total leakage-out signal is the difference between the input volume-change and the landmass value.

4.2. A More Advanced Simulation (the Arctic Region)

[42] The second simulation study is composed of an investigation of both leakage-out and leakage-in effects, embedded in a close-to-reality configuration of mass changes. Again, the initial total mass change over Greenland is -500 km^3. However, we additionally consider disturbing signals, as outlined in Table 2. Figure 7 presents the corresponding gravitational potential forward modeling result as input for the four-step procedure. Keep in mind that the disturbing signals are both negative (Alaska) and positive (Canadian Shield and Fennoscandia).

4.2.1. Steps 1–4

[43] We perform the first three steps of this simulation as for the first simulation study in section 4.1. In order to quantify the true leakage-in effect at a later stage, we use the same extended areas as before, see Figure 6. According to Table 4, both the volume-change estimate over Greenland itself (-299.6 km^3) and the results for the extended areas become smaller, which is due to leakage-in effects. As they affect all regions similarly, the IAFs are similar to the values in Table 3.

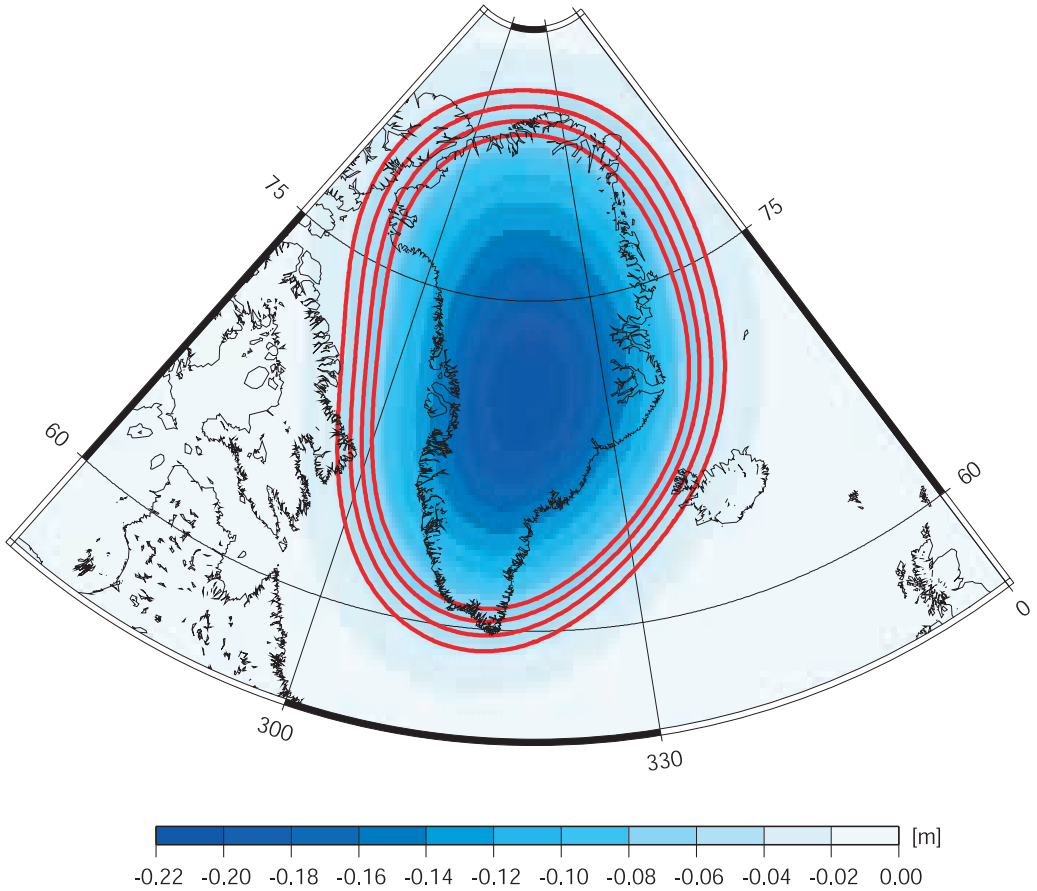

Figure 6. Definition of extended areas for simulation study 1 over the Greenland region, in terms of EWT isolines [Albers projection].

[44] Again, the IAF is used to restore the leakage-out signal from the extended area back onto land. In the fourth step, forward modeling provides the signal loss due to signal leaking beyond the extended area. The sum of the volume-change estimate inside the extended area and the signal loss amounts to the total volume-change $M_{1,\mathrm{syn}}$. Numerical values are given in the fifth column of Table 4 all are considerably smaller than the initial volume-change input (-500 km^3). In other words, within the range of 4%, the model errors are much higher than in the first simulation study. This is simply because leakage-in effects have not been reduced thus far.

4.2.2. Leakage-in

[45] To account for leakage-in effects, the impact of each single disturbing source, i.e., Alaska (ALA), the Canadian Shield (CAN) and Fennoscandia (FEN) has to be isolated by applying the procedure to each. Opposed to the quantification of leakage-out effects, however, the leakage-in signal is obtained by evaluating the volume-change signal of the disturbing source in the region of interest, i.e., Greenland. Table 5 displays the results for each individual disturbing source, as well as the total effect.

[46] Considering leakage-in, the model errors reduce to 1–2%. It is important to mention that the total leakage-in signal is positive, thus dominated by the positive GIA signal over the Canadian Shield. The further contributions have a lesser impact. Hence reducing leakage-in effects over Greenland results in an increase of the total volume result. As a consequence, the FAFs in Table 5 are greater than for the first simulation study.

[47] Finally, Table 6 summarizes both the true and estimated signal loss (or additional leakage-out) and leakage-in values. The true signal loss is provided by the first simulation study by subtracting the volume-change within the extended area from the initial volume-change input. Accordingly, in this second study, the true leakage-in signal is derived by subtracting both the signal loss and the volume-change estimate within the extended area from the initial value. The overall error

Table 3. Simulation Study 1: Volume-Change Magnitudes and Amplification Factors for Different Extended Areas[a]

Region	M_2 (km^3)	IAF	Signal Loss (%)	$M_{1,\mathrm{syn}}$ (km^3)	FAF	Error (%)
Land	−305.2	1.00	–	–	–	–
Isoline −0.07 m	−401.5	1.32	22.6	−492.1	1.61	1.58
Isoline −0.06 m	−427.1	1.40	15.6	−493.7	1.62	1.27
Isoline −0.05 m	−453.0	1.48	9.2	−494.4	1.62	1.11
Isoline −0.04 m	−477.9	1.57	3.7	−495.7	1.62	0.87

[a]Initial volume-change input: −500 km^3.

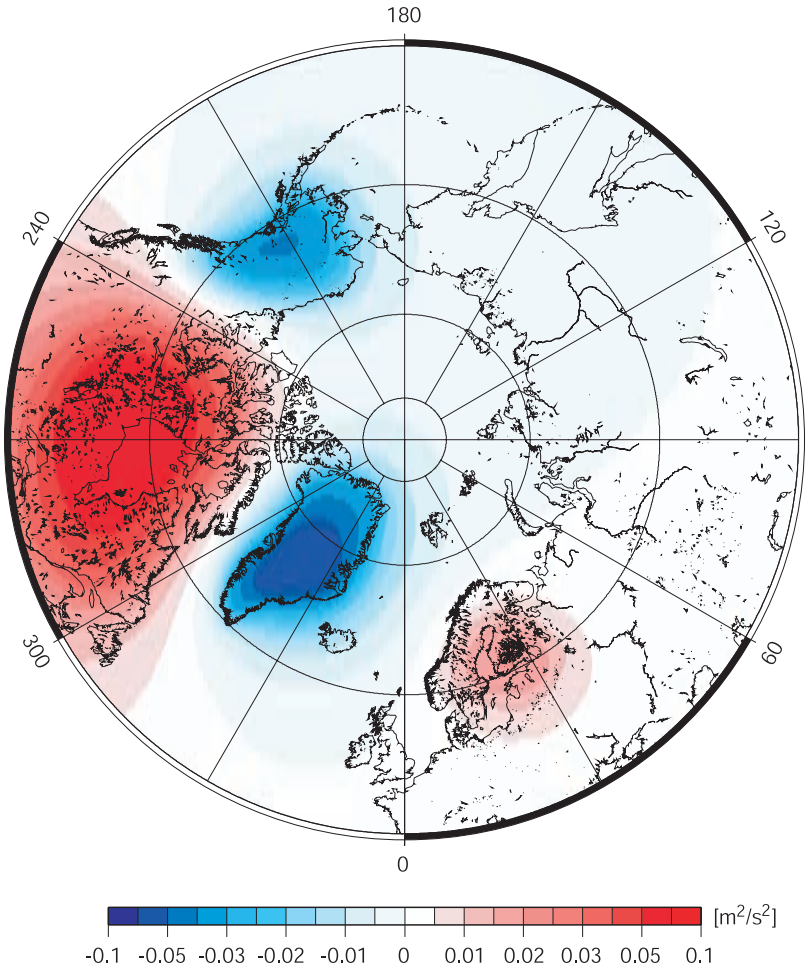

Figure 7. Input for the second simulation study: forward modeled potential signal [Azimuthal projection].

budget (last column in Table 6) is dominated by errors in leakage-out modeling.

5. Recent GRACE-Derived Ice-Mass Changes Over Greenland

[48] In order to derive the 2002–2008 ice-mass balance over Greenland, we apply our procedure to the GRACE patterns displayed in Figure 4. As demonstrated in section 4, the choice of extended areas has only a minor impact on the secular trend estimation process. Hence we only present the results using the extended areas performing best within the simulation studies, that is, we restrict ourselves to the contour lines in Figure 4.

[49] Depending on the smoothing radius used for spatial averaging, Table 7 summarizes the results of the individual computation steps for the GRACE gravity field solutions provided by CSR, GFZ and JPL from August 2002 to July 2008 (inclusive). The third column provides the ice-volume changes over the Greenland landmass. The estimate within the extended area (outer contour line in Figure 6) is expressed in terms of the IAF (fourth column), i.e., the ratio between the estimate inside the extended area and the

Table 4. Simulation Study 2: Volume-Change Magnitudes and Amplification Factors for Different Extended Areas[a]

Region	M_2 (km^3)	IAF	Signal Loss (%)	$M_{1,syn}$ (km^3)	FAF	Error (%)
Land	−299.6	1.00	–	–	–	–
Isoline −0.07 m	−392.2	1.31	22.5	−480.3	1.60	3.94
Isoline −0.06 m	−416.4	1.39	15.5	−480.8	1.60	3.84
Isoline −0.05 m	−440.0	1.47	9.1	−480.0	1.60	4.00
Isoline −0.04 m	−462.3	1.54	3.7	−479.2	1.60	4.15

[a]Greenland initial mass-change input: −500 km^3. Only the leakage-out effect is considered.

Table 5. Simulation Study 2: Volume-Change Magnitudes and Amplification Factors for Different Extended Areas[a]

	Leakage-in (km^3)					
Region	ALA	CAN	FEN	Total	FAF	Error (%)
Isoline −0.07 m	−0.6	8.9	0.7	9.0	1.63	2.14
Isoline −0.06 m	−0.7	10.3	0.8	10.4	1.64	1.76
Isoline −0.05 m	−0.8	12.4	0.9	12.5	1.64	1.50
Isoline −0.04 m	−0.9	15.0	1.0	15.1	1.65	1.14

[a]Greenland initial mass-change input: −500 km^3. Both leakage-out and leakage-in effects are considered.

Table 6. Simulation Study 2: True and Estimated Signal Loss and Leakage-in Values for Different Extended Areas[a]

Extended Area	Signal Loss (km^3)			Leakage-in (km^3)			Total Error (%)
	True	Estimate	Error (%)	True	Estimate	Error (%)	
Isoline −0.07 m	−98.5	−88.1	2.1	9.3	9.0	0.1	2.14
Isoline −0.06 m	−72.9	−64.4	1.7	10.7	10.4	0.1	1.76
Isoline −0.05 m	−47.0	−40.0	1.4	13.0	12.5	0.1	1.50
Isoline −0.04 m	−22.1	−16.9	1.0	15.6	15.1	0.1	1.14

[a]Greenland initial mass-change input: −500 km^3.

value derived over landmass. The signal loss in column five quantifies the leakage-out signal spreading beyond the limited extended area definition. Hence it accounts for the additional leakage-out effect. The sixth column displays the effect of leakage-in signals caused by Alaska, the Canadian Shield and Fennoscandia.

[50] As highlighted in section 4.2, the overall leakage-in effect is dominated by the strong positive GIA signal over the Canadian Shield. For all scenarios in Table 7, it amounts to roughly 100% of the total leakage-in effect; Alaska only contributes about −10% and Fennoscandia about 10%. In this context, the correction for leakage-in effects is performed by algebraic subtraction. Finally, the FAF incorporates all leakage-out and leakage-in effects. Multiplied by the initial volume-change over landmass, it provides the total ice-volume change; see the last column in Table 7. Most notably, the FAF reveals that without taking leakage effects into account, mass-change amplitudes over Greenland are reduced by about 50%, i.e., a factor of 2.

[51] As the initial estimate over landmass depends on the smoothing radius R, the FAFs differ accordingly. They increase with increasing R, which is due to the reduction of signal power for increased smoothing. Independent from the smoothing radius applied, for each processing center individually, the ablation rates over Greenland are in very good agreement. From the smallest to the largest values, they vary by a few percent only. Our method is therefore largely insensitive toward the degree of Gaussian smoothing. The accuracy of the estimates, however, reduces dramatically with decreasing R. The results presented in Table 7 suggest an optimal (least uncertainty) of about 500 km for the CSR and GFZ solution and a larger radius for the JPL solution. Taking the average over all smoothing radii, the annual ice-volume loss becomes -242 ± 14 km^3 a^{-1} (CSR), -194 ± 24 km^3 a^{-1} (GFZ) and -96 ± 23 km^3 a^{-1} (JPL) respectively. Note that these values are free of any GIA correction.

[52] On the other hand, analysis of the gravity field solutions provided by CSR, GFZ and JPL exhibit a significant spread. This is a straightforward outcome from the trend patterns in Figure 4, as the mass change over Greenland is clearly smallest in magnitude for JPL. As long as the discrepancies among the various GRACE solutions can be explained, we recommend to average the individual results, finally yielding the ice-volume decline to become -177 ± 12 km^3 a^{-1}.

[53] Table 8 highlights ablation rates of the Greenland area derived by different GRACE-based studies. The values reveal a rather large spread among the different studies, ranging from -87 ± 23 km^3 a^{-1} to -242 ± 14 km^3 a^{-1}, well exceeding the formal errors given. As such, the interpretation of the change rates from these data has to be done cautiously. Accelerated melting could be one reason for the rising secular trend, especially when compared to pre-GRACE estimates. However, the application of different analysis methods to different series of gravity field solutions, in combination with inconsistent survey periods, make the values difficult to compare. Part of the spread may be explained by the way leakage is considered within the individual studies. As our amplification factors demonstrate, the leakage signal amounts to about 50% of the total mass change over Greenland. Variations in the treatment of leakage effects significantly impact mass balance results.

6. Discussion

[54] The separation of GRACE-detected gravity signals from GRACE measurement errors is one of the major challenges with regard to the accurate estimation of temporal mass variations. High-degree GRACE-derived coefficients are contaminated by large errors. Despite the

Table 7. GRACE-Derived Total Ice-Volume Variations From August 2002 to July 2008 (Inclusive), Dependent on Both the GRACE Data Processing Center and Gaussian Smoothing[a]

Processing Center	Radius R (km)	Landmass (km^3)	IAF	Signal Loss (km^3)	Leakage-in (km^3)	FAF	Total Change (km^3)
CSR	200	−801.6	1.98	135.3	15.6	1.83	−1468.2 ± 228.8
	300	−781.3	1.94	91.1	16.0	1.85	−1447.0 ± 192.6
	400	−751.3	1.92	22.7	17.5	1.92	−1440.5 ± 176.0
	500	−713.6	1.91	−67.4	19.1	2.03	−1449.3 ± 169.8
	600	−670.3	1.90	−172.8	21.7	2.19	−1469.9 ± 170.2
GFZ	200	−673.0	1.92	106.9	18.1	1.79	−1204.3 ± 587.9
	300	−645.2	1.91	75.2	18.2	1.82	−1174.8 ± 296.1
	400	−612.4	1.89	21.9	19.7	1.88	−1153.2 ± 196.2
	500	−573.9	1.87	−47.4	22.7	1.99	−1143.9 ± 169.4
	600	−531.3	1.86	−127.7	27.3	2.16	−1145.2 ± 166.2
JPL	200	−264.6	2.42	54.9	14.9	2.27	−600.5 ± 576.2
	300	−265.7	2.31	44.4	15.5	2.20	−584.0 ± 275.4
	400	−264.3	2.17	20.8	17.1	2.16	−569.6 ± 168.8
	500	−257.7	2.05	−12.5	19.9	2.18	−561.9 ± 131.5
	600	−245.6	1.97	−52.0	24.2	2.28	−559.8 ± 116.0

[a]No GIA correction applied.

Table 8. Results of Ice-Volume Change Rates Over the Greenland Area Obtained by GRACE Gravimetry

Study	Survey Period	Ice-Volume Change Rate ($km^3\ a^{-1}$) Without GIA	With GIA
Velicogna and Wahr [2005]	April 2002–July 2004	−87 ± 23	−82 ± 28
Ramillien et al. [2006]	July 2002–March 2005	−130 ± 11	−141 ± 16
Velicogna and Wahr [2006b]	April 2002–April 2006	−240 ± 12	−248 ± 36
Chen et al. [2006b]	April 2002–November 2005	−239 ± 23	−234 ± 24
Luthcke et al. [2006]	July 2003–July 2005	−103 ± 17	−110 ± 17
This study	CSR August 2002–July 2008	−242 ± 14	–
	GFZ August 2002–July 2008	−194 ± 24	–
	JPL August 2002–July 2008	−96 ± 23	–
	Average August 2002–July 2008	−177± 12	–

damping of short wavelength spectral components, non-reduced GRACE errors still affect the numerical results. As such, the performance of our procedure with regard to both simulated and real-data scenarios depends on the GRACE error budget.

[55] The principle of rescaling mass-change estimates within an area of interest in order to restore realistic amplitudes has been adopted in several investigations [e.g., *Swenson and Wahr*, 2002; *Seo and Wilson*, 2005; *Velicogna and Wahr*, 2005; *Chen et al.*, 2006b]. Typically, these studies consider the total leakage signal in the target area at once. They neither isolate nor quantify individual disturbing sources present in the GRACE signal.

[56] Opposed to earlier studies, the benefit of our procedure is twofold. First, it allows the systematic classification of the complex nature of leakage effects. We split up the total leakage signal in its (major) individual parts. In this context, the separation between leakage-in and leakage-out is of importance for the full understanding of the problem. For mass-change balance over Greenland, it turns out that leakage-in effects are of minor importance. However, the composition of superposed individual signals strongly depends on the region of interest, i.e., the geographical position. In regions other than Greenland, leakage-in might dominate to leakage-out. Secondly, recalling steps 2 and 3, we want to highlight that the forward modeling step is based on more realistic mass-change magnitudes as opposed to neglecting these intermediate steps.

[57] Scrutinizing GRACE-derived mass balance results provided in Table 8 show that, so far, there is no clear consensus about the magnitude of present ice-mass decline over Greenland. On the other hand, the numbers given are based on highly inconsistent conditions. They are neither the outcome of the same survey period nor incorporate the same release of gravity field solutions. Consequently, it is not possible to evaluate the analysis methods with regard to performance. Nonetheless, we suspect that the correction for leakage effects to be partly responsible for the discrepancies. The reconcilement of the results would require the different approaches to be applied to a consistent data set. Even though we consider this matter to be urgent, this reconcilement lies beyond the scope of this paper.

[58] In any case, the comparison of different GRACE-derived results is strongly biased. Only the comparison with independent data, such as provided by InSAR (Interferometric synthetic aperture radar), allows one to evaluate change-rate numbers objectively. As reported by *Rignot and Kanagaratnam* [2006], InSAR data from 2005 show the ablation rate over Greenland to be $-224 \pm 41\ km^3\ a^{-1}$. This result is very comparable with GRACE. In particular, it is in very good agreement with the secular trends obtained by *Velicogna and Wahr* [2006b], *Chen et al.* [2006b] and our results.

7. Conclusions

[59] In an attempt to derive more reliable secular mass-change trends from GRACE satellite gravimetry, we have devised a four-step analysis procedure, followed by two simulations and application to 6 whole years of GRACE data over Greenland from three different analysis centers. The four-step method is characterized by the separation of individual leakage sources; it allows the quantification of both leakage-out and leakage-in signals. The former are much higher in magnitude (about one order) than the latter over Greenland. The leakage-in effect is dominated by the strong GIA signal over the Canadian Shield. Most notably, without taking leakage effects into account, mass-change amplitudes over Greenland would be reduced by about 50%.

[60] Our analysis of RL04 GRACE level 2 data over the 6-year period from August 2002 to July 2008 (inclusive) shows an annual ice-mass decline over Greenland of $-177 \pm 12\ km^3\ a^{-1}$. We identify that other GRACE-derived deglaciation rates are strongly dependent on the series of gravity field solutions used. In order to derive our GRACE-based secular trend, we simply averaged the results applied to data from different analysis centers: CSR ($-242 \pm 14\ km^3\ a^{-1}$), GFZ ($-194 \pm 24\ km^3\ a^{-1}$) and JPL ($-96 \pm 23\ km^3\ a^{-1}$). Note that these values do not account for GIA corrections, but which are more than one order of magnitude smaller.

[61] Our change-rate results are in very good agreement with alternative GRACE studies and recent, independent, InSAR measurements. We want to point out, however, that each study is characterized by its individual analysis method, underlying series of gravity field solutions, and survey period. The different conditions make the change-rate numbers difficult to compare objectively.

[62] **Acknowledgments.** This project was funded by Australian Research Council Discovery Project grant DP0345583. This is TIGeR publication number 182. We kindly acknowledge helpful comments by two anonymous reviewers of the manuscript.

References

Chambers, D. P. (2006a), Observing seasonal steric sea level variations with GRACE and satellite altimetry, *J. Geophys. Res.*, *111*, C03010, doi:10.1029/2005JC002914.

Chambers, D. P. (2006b), Evaluation of new GRACE time-variable gravity data over the ocean, *Geophys. Res. Lett.*, *33*, L17603, doi:10.1029/2006GL027296.

Chambers, D. P., M. E. Tamisiea, R. S. Nerem, and J. C. Ries (2007), Effects of ice melting on GRACE observations of ocean mass trends, *Geophys. Res. Lett.*, *34*, L05610, doi:10.1029/2006GL029171.

Chen, J. L., B. D. Tapley, and C. R. Wilson (2006a), Alaskan mountain glacial melting observed by satellite gravimetry, *Earth Planet. Sci. Lett.*, *248*, 368–378.

Chen, J. L., C. R. Wilson, and B. D. Tapley (2006b), Satellite gravity measurements confirm accelerated melting of Greenland ice sheet, *Science*, *313*, 1958–1960, doi:10.1126/science.1129007.

Chen, J. L., C. R. Wilson, D. D. Blankenship, and B. D. Tapley (2006c), Antarctic mass rates from GRACE, *Geophys. Res. Lett.*, *33*, L11502, doi:10.1029/2006GL026369.

Dobslaw, H., and M. Thomas (2007), Simulation and observation of global ocean mass anomalies, *J. Geophys. Res.*, *112*, C05040, doi:10.1029/2006JC004035.

Farrell, W. E. (1972), Deformation of the Earth by surface loads, *Rev. Geophys.*, *10*, 761–797.

Han, S. C., C. K. Shum, C. Jekeli, and D. Alsdorf (2005a), Improved estimation of terrestrial water storage changes from GRACE, *Geophys. Res. Lett.*, *32*, L07302, doi:10.1029/2005GL022382.

Han, S. C., C. K. Shum, C. Jekeli, C. Y. Kuo, C. Wilson, and K. W. Seo (2005b), Non-isotropic filtering of GRACE temporal gravity for geophysical signal enhancement, *Geophys. J. Int.*, *163*, 1825, doi:10.1111/j.1365-246X.2005.02756.x.

Heiskanen, W. A., and H. Mortiz (1967), *Physical Geodesy*, W. H. Freeman, San Francisco, Calif.

Jekeli, C. (1981), Alternative methods to smooth the Earth's gravity field, *Rep. 327*, Dep. of Geod. Sci. and Surv. Ohio State Univ., Columbus.

Lombard, A., D. Garcia, G. Ramillien, A. Cazenave, R. Biancale, J. M. Lemoine, F. Flechtner, R. Schmidt, and M. Ishii (2007), Estimation of steric sea level variations from combined GRACE and Jason-1 data, *Earth Planet. Sci. Lett.*, *254*, 194–202, doi:10.1016/j.epsl.2006.11.035.

Luthcke, S. B., H. J. Zwally, W. Abdalati, D. D. Rowlands, R. D. Ray, R. S. Nerem, F. G. Lemoine, J. J. McCarthy, and D. S. Chinn (2006), Recent Greenland ice mass loss by drainage system from satellite gravity observations, *Science*, *314*, 1286–1289, doi:10.1126/science.1130776.

Peltier, W. R., and J. T. Andrew (1976), Glatial isostatic adjustment. I: The forward problem, *Geophy. J. R. Astron. Soc.*, *46*, 605–646.

Ramillien, G., F. Frappart, A. Cazenave, and A. Güntner (2005), Time variations of land water storage from an inversion of 2 years of GRACE geoids [rapid communication], *Earth Planet. Sci. Lett.*, *235*, 283–301, doi:10.1016/j.epsl.2005.04.005.

Ramillien, G., A. Lombart, A. Cazenave, E. R. Ivins, M. Llubes, F. Remy, and R. Biancale (2006), Interannual variations of the mass balance of the Antarctica and Greenland ice sheets from GRACE, *Global Planet. Change*, *53*, 198–208, doi:10.1016/j.gloplacha.2006.06.003.

Rignot, E., and P. Kanagaratnam (2006), Changes in the velocity structure of the Greenland ice sheet, *Science*, *311*, 986–990, doi:10.1126/science.1121381.

Seo, K.-W., and C. R. Wilson (2005), Simulated estimation of hydrological loads from GRACE, *J. Geod.*, *78*, 442–456, doi:10.1007/s00190-004-0410-5.

Swenson, S., and J. Wahr (2002), Methods for inferring regional surface-mass anomalies from Gravity Recovery and Climate Experiment (GRACE), measurements of time-variable gravity, *J. Geophys. Res.*, *107*(B9), 2193, doi:10.1029/2001JB000576.

Swenson, S., and J. Wahr (2006), Post-processing removal of correlated errors in GRACE data, *Geophys. Res. Lett.*, *33*, L08402, doi:10.1029/2005GL025285.

Swenson, S., J. Wahr, and P. C. D. Milly (2003), Estimated accuracies of regional water storage variations interfered from the Gravity Recovery and Climate Experiment (GRACE), *Water Resour. Res.*, *39*(8), 1223, doi:10.1029/2002WR001808.

Tamisiea, M. E., E. W. Leuliette, J. L. Davis, and J. X. Mitrovica (2005), Constraining hydrological and cryospheric mass flux in southeastern Alaska using space-based gravity measurements, *Geophys. Res. Lett.*, *32*, L20501, doi:10.1029/2005GL023961.

Tapley, B. D., S. Bettadpur, M. Watkins, and C. Reigber (2004a), The gravity recovery and climate experiment: Mission overview and early results, *Geophys. Res. Lett.*, *31*, L09607, doi:10.1029/2004GL019920.

Tapley, B. D., D. Bettadpur, J. C. Ries, P. F. Thompson, and M. M. Watkins (2004b), GRACE measurements of mass variability in the earth system, *Science*, *305*, 503–505, doi:10.1126/science.1099192.

Velicogna, I., and J. Wahr (2005), Greenland mass balance from GRACE, *Geophys. Res. Lett.*, *32*, L18505, doi:10.1029/2005GL023955.

Velicogna, I., and J. Wahr (2006a), Measurements of time-variable gravity show mass loss in Antarctica, *Science*, *311*, 1754–1756, doi:10.1126/science.1123785.

Velicogna, I., and J. Wahr (2006b), Acceleration of Greenland ice mass loss in spring 2004, *Nature*, *443*, 329–331, doi:10.1038/nature05168.

Velicogna, I., J. Wahr, E. Hanna, and P. Huybrechts (2005), Short term mass variability in Greenland, from GRACE, *Geophys. Res. Lett.*, *32*, L05501, doi:10.1029/2004GL021948.

Wagner, C., D. McAdoo, J. Klokoèník, and J. Kostelecký (2006), Degradation of geopotential recovery from short repeat-cycle orbits: Application to GRACE monthly fields, *J. Geod.*, *80*, 94–103, doi:10.1007/s00190-006-0036-x.

Wahr, J., M. Molenaar, and F. Bryan (1998), Time variability of the Earth's gravity field: Hydrological and oceanic effects and their possible detection using GRACE, *J. Geophys. Res.*, *103*, 30,205–30,229.

O. Baur, Institute of Geodesy, Universität Stuttgart, Geschwister-Scholl-Straße 24D, D-70174 Stuttgart, Germany. (baur@gis.uni-stuttgart.de)

W. E. Featherstone and M. Kuhn, Western Australian Centre for Geodesy and Institute for Geoscience Research, Curtin University of Technology, GPO Box U1987, Perth, WA 6845, Australia. (w.featherstone@curtin.edu.au; m.kuhn@curtin.edu.au)